nature neuroscience

Chordin-induced lineage plasticity of adult SVZ neuroblasts after demyelination

Beata Jablonska[1,5], Adan Aguirre[1,5], Matthew Raymond[1,2], Gabor Szabo[3], Yasuji Kitabatake[4], Kurt A Sailor[4], Guo-Li Ming[4], Hongjun Song[4] & Vittorio Gallo[1]

The mechanisms that regulate the developmental potential of adult neural progenitor populations under physiological and pathological conditions remain poorly defined. Glutamic acid decarboxylase 65 (GAD65)- and Doublecortin (Dcx)-expressing cells constitute major progenitor populations in the adult mouse subventricular zone (SVZ). Under normal physiological conditions, SVZ-derived GAD65-positive and Dcx-positive cells expressed the transcription factor Pax6 and migrated along the rostral migratory stream to the olfactory bulb to generate interneurons. After lysolecithin-induced demyelination of corpus callosum, however, these cells altered their molecular and cellular properties and migratory path. Demyelination upregulated chordin in the SVZ, which redirected GAD65-positive and Dcx-positive progenitors from neuronal to glial fates, generating new oligodendrocytes in the corpus callosum. Our findings suggest that the lineage plasticity of SVZ progenitor cells could be a potential therapeutic strategy for diseased or injured brain.

In adult brain, the SVZ of the lateral ventricle and subgranular zone (SGZ) of the hippocampal dentate gyrus maintain sources of neural stem cells and neural progenitor cells (NPCs)[1–5]. NPCs of the SVZ retain mitotic and differentiation potential throughout their lifespan, as the brain is able to replenish damaged glia and neurons through endogenous gliogenesis and neurogenesis[6,7]. GAD65- and Dcx-expressing cells constitute major NPC populations in adult SVZ and normally migrate along the rostral migratory stream (RMS) toward the olfactory bulb, generating inhibitory interneurons[8]. In SVZ and RMS, NPCs committed to generating interneurons can be identified by the expression of Dcx, Pax6 and GAD65 (refs. 9,10).

The SVZ also generates oligodendrocytes under physiological and pathological conditions[11–15]. In postnatal and adult brain, NPCs that generate oligodendrocytes migrate from SVZ to developing white matter, where they stop dividing, differentiate and myelinate axons[16,17]. This process recurs after white-matter demyelination[11,13–15]. Identifying the molecular signals that regulate the differentiation potential of SVZ NPCs would provide information about oligodendrocyte repair strategies directed at endogenous NPCs.

A recent study found that hippocampal NPCs change their fate potential to generate oligodendrocytes, rather than neurons, after retroviral-mediated overexpression of the bHLH transcription factor Ascl1 (Mash1)[18]. Whether this process occurs in native progenitors under normal or pathological conditions is unknown. Furthermore, the cellular signals promoting oligodendrogenesis by upregulating Mash1 in NPCs remain unidentified. We performed focal demyelination[14,19] in adult corpus callosum of transgenic mice expressing green

fluorescent protein (GFP) under the control of the *Gad2* (*Gad65*) or *Dcx* promoters[10,20] (these are referred to as GAD65-GFP– and Dcx-GFP–positive NPCs, respectively) to investigate whether demyelination stimulates lineage plasticity of SVZ NPCs. These mouse strains allowed us to monitor proliferation, migration and differentiation of GAD65-GFP–positive and Dcx-GFP–positive NPCs. We found that demyelination induced GAD65- and Dcx-expressing NPCs of adult SVZ to generate oligodendrocytes, rather than neurons, in corpus callosum. In addition, the bone morphogenetic protein (BMP) antagonist chordin induced lineage plasticity in these NPC populations after demyelination.

RESULTS

GAD65+ cells generate oligodendrocytes after demyelination

We characterized GAD65-GFP–expressing cells in the SVZ and RMS of adult (postnatal days 40–60, P40–60) GAD65-GFP mice using various neuronal and glial cell markers. Most GAD65-GFP–positive cells in the SVZ and RMS had a neuroblast phenotype, expressing cellular markers of olfactory bulb interneuron progenitors, including Dcx and Pax6 (**Supplementary Fig. 1**). Although most GAD65-GFP–positive cells expressed neuronal markers in SVZ and RMS, a low percentage expressed Mash1 or NG2 (**Supplementary Fig. 1**) and a small percentage of GAD65-GFP–positive cells expressed oligodendrocytic markers, including Nkx2.2 and Olig2 (**Supplementary Fig. 1**). Virtually all of the GAD65-GFP–positive, Olig2-positive cells also expressed Mash1, but none coexpressed Pax6 (data not shown). Finally, some GAD65-GFP–positive, Dcx-positive neuroblasts in SVZ coexpressed Pax6 and Dlx2 ($5.6 \pm 0.09\%$

and 5.4 ± 0.9%, respectively); however, we found no GAD65-GFP–positive, Dcx-positive cells that coexpressed Olig2.

Immunohistochemistry data were validated by reverse transcription PCR (RT-PCR) from fluorescence-activated cell sorting (FACS)-purified GAD65-GFP–positive cells. As expected, mRNAs for *Map2* and *Gad2* were abundant in these cells (**Supplementary Fig. 1**), whereas levels of *Olig2*, *Ascl1*, *NG2* (also known as *Cspg4*) and *Gfap* mRNAs were

low (**Supplementary Fig. 1**). *In vitro* cultures of GAD65-GFP–positive cells that were FACS purified from the SVZ of adult GAD65-GFP mice confirmed their neuronal fate. After 1 or 5 d in culture, no GFP-positive cells expressed the oligodendrocyte markers Olig2 or galactocerebroside (GalC) or the astrocyte marker GFAP (**Supplementary Fig. 1**). After 5 d in culture, 100% of GAD65-GFP–positive cells had differentiated into mature MAP2-positive neurons (**Supplementary Fig. 1**).
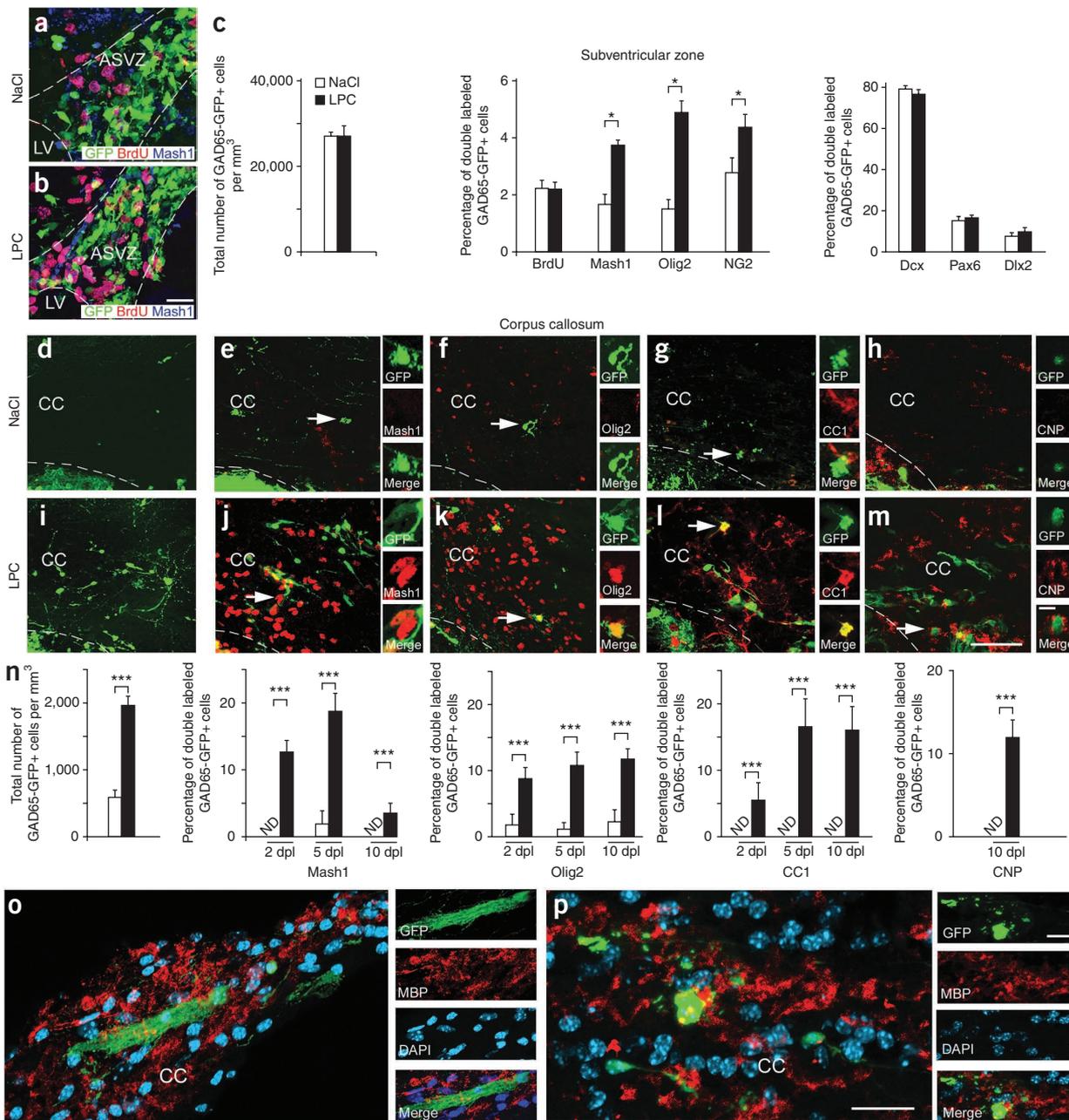
Figure 1 Demyelination increases GAD65-GFP–positive cells expressing glial lineage markers in the SVZ and corpus callosum. (**a,b**) GAD65-GFP–positive cells in the anterior subventricular zone (ASVZ) immunolabeled with antibodies to BrdU and Mash1 after NaCl (**a**) or LPC (**b**) injection at 5 dpl. Dotted lines bound ASVZ and lateral ventricle (LV). Scale bar represents 50 µm. (**c**) Total number of GAD65-GFP–positive cells does not change after LPC injections (*n* = 8 brains). Percentages of double-labeled GAD65-GFP–positive cells stained with antibodies to BrdU, Mash1, Olig2, NG2, Dcx, Pax6 and Dlx2 after LPC injections (*n* = 4 brains, **P* < 0.05, *t* test). (**d–m**) Images of GAD65-GFP–positive cells in NaCl-injected (**d–h**) and LPC-injected (**i–m**) corpus callosum (CC) at 10 dpl. Cells were colabeled with antibodies to Mash1 (**e,j**), Olig2 (**f,k**), CC1 (**g,l**) or CNP (**h,m**). Dotted lines bound corpus callosum. Insets magnify cells indicated by arrows. Scale bar represents 50 µm. (**n**) Density of GAD65-GFP–positive cells in LPC- and NaCl-injected corpus callosum. Shown are the percentages of GAD65-GFP–positive and Mash1-positive, GAD65-GFP–positive and Olig2-positive, GAD65-GFP–positive and CC1-positive, and GAD65-GFP–positive and CNP-positive cells in LPC- and in NaCl-injected corpus callosum. ND, not detectable. Bar graphs represent means ± s.e.m. (*n* = 4–8 brains, ****P* < 0.02, *t* test). (**o,p**) Images of GAD65-GFP–positive cells in LPC-injected corpus callosum at 14 dpl. GAD65-GFP–positive, MBP-positive oligodendrocytes were detected only in LPC-injected corpus callosum. Scale bars represent 50 µm.

Figure 2 Demyelination alters the migratory pathway and phenotype of GAD65-GFP–positive cells. (**a**) Confocal images of a sagittal brain section showing migratory pathway of GAD65-GFP–positive progenitor cells from the SVZ to the olfactory bulb (OB) along the RMS. Under normal conditions, GAD65-GFP–positive cells were found exclusively in the olfactory bulb; none migrated to the corpus callosum. Scale bar represents 400 μm. (**b**) Magnification of RMS GAD65-GFP–positive cells in white boxes, showing their neuronal morphology. Scale bar represents 20 μm. (**c**–**e**) At 14 dpl GAD65-GFP–positive cells in demyelinated corpus callosum coexpressed Mash1, Olig2 and CC1, but not Pax6. White arrowheads indicate GAD65-GFP–positive cells colabeled with different markers. Scale bar represents 20 μm. (**f**) Images show GAD65-GFP–positive cells immunolabeled with antibody to MBP in demyelinated corpus callosum at 14 dpl. CTX, cerebral cortex. Scale bar represents 400 μm. (**g**) Higher magnification of GAD65-GFP–positive cells colabeled with antibody to MBP in demyelinated corpus callosum. Scale bar represents 400 μm.

To determine whether GAD65-GFP–positive cells of adult SVZ could generate glia, rather than neurons, under pathological conditions, we analyzed these cells after lysolecithin (LPC)-induced demyelination of corpus callosum. We characterized GAD65-GFP–positive cells in SVZ and corpus callosum 2, 5 and 10 d after LPC-induced demyelination (days post-lesion, dpl). The total number of GAD65-GFP–positive cells at 5 dpl in SVZ was unchanged compared to the NaCl-injected contralateral side (**Fig. 1a**). Consistent with previous observations[6], the total number of BrdU-positive cells in SVZ increased by 5 dpl (**Fig. 1a,b**); however, the percentage of GAD65-GFP–positive, BrdU-positive cells remained unchanged (**Fig. 1c**). Conversely, percentages of GAD65-GFP–positive and Mash1-positive, GAD65-GFP–positive and Olig2-positive, and GAD65-GFP–positive and NG2-positive cells increased significantly after LPC injection compared with NaCl injection ($P < 0.05$; **Fig. 1c**). There were no substantial changes in the percentages of GAD65-GFP–positive and Dcx-positive, GAD65-GFP–positive and Pax6-positive, or GAD65-GFP–positive and Dlx2-positive cells (**Fig. 1c**). Finally, the percentage of GAD65-GFP–positive and Dcx-positive neuroblasts coexpressing Pax6 and Dlx2 was not substantially different after LPC injection compared with NaCl injection. (**Supplementary Fig. 2**). GAD65-GFP–positive and Dcx-positive cells coexpressing Olig2 were not detected after LPC-induced demyelination (data not shown). Overall, our data indicate that a demyelinating insult does not alter the overall number of GAD65-GFP–positive cells in the adult SVZ, but does enhance the expression of oligodendroglial progenitor markers in this population.

We next looked for GAD65-GFP–positive cells in the demyelinated corpus callosum lesion. Significantly more GAD65-GFP–positive cells were found in the corpus callosum after demyelination than in NaCl-injected hemispheres ($P < 0.02$; **Fig. 1d,i,n**). Immunohistochemical staining with specific antibodies confirmed that GAD65-GFP–positive cells in demyelinated corpus callosum also expressed GAD65/67 protein (data not shown). GAD65-GFP–positive cells in demyelinated corpus callosum were characterized by various cellular markers, including Mash1, Olig2, CC1 and CNP. The percentage of GAD65-GFP–positive and Mash1-positive progenitor cells increased from 2 to 5 dpl, then fell significantly by 10 dpl ($P < 0.02$; **Fig. 1e,j,n**). Conversely, the percentages of GAD65-GFP–positive and Olig2-positive and GAD65-GFP–positive and CC1-positive oligodendrocytes continued increasing until 10 dpl ($P < 0.02$; **Fig. 1f,k,g,l,n**). At 10 dpl, a significant percentage of GAD65-GFP–positive cells also expressed CNP, indicating that they had differentiated into mature oligodendrocytes (**Fig. 1h,m,n**), consistent with the observation that GAD65-GFP–positive cells in demyelinated lesions displayed typical oligodendrocyte (multipolar and large cell body), rather than neuroblast, morphology (leading cell process and small cell body;
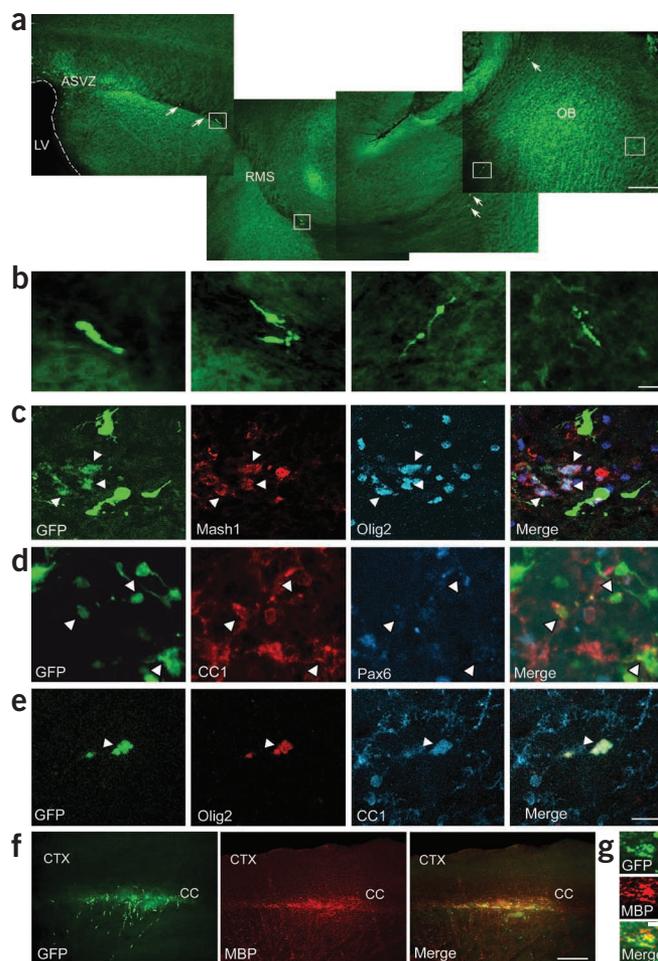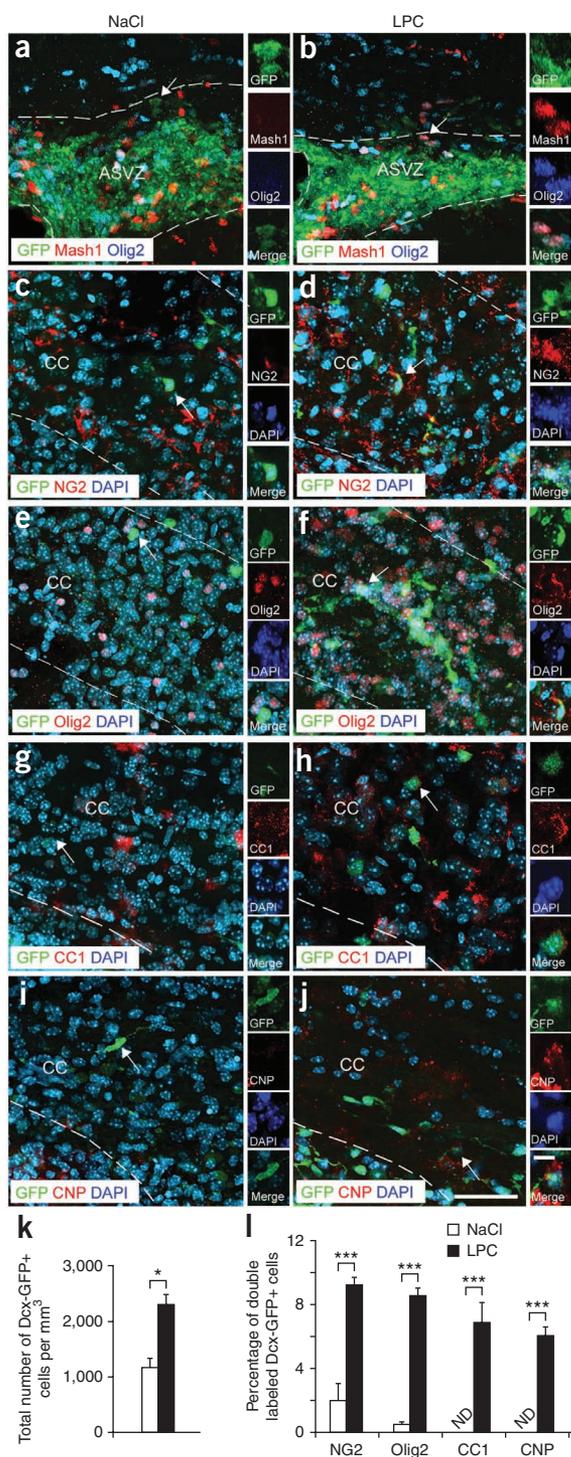
Fig. 1d–m). At 10 dpl, a substantial percentage of GAD65-GFP–positive cells in the demyelinated lesions expressed myelin basic protein (MBP; **Fig. 1o,p**) and often displayed bundles of cellular processes typical of myelinating oligodendrocytes (**Fig. 1o**). In demyelinated corpus callosum, GAD65-GFP–positive cells in the lesion did not express the neuronal markers MAP2 and Dcx (data not shown). We found no apoptotic GAD65-GFP–positive oligodendrocytes in demyelinated corpus callosum by 30 dpl (data not shown). These results indicate that GAD65-GFP–positive cells in demyelinated corpus callosum express markers of the oligodendrocyte lineage and differentiate into mature oligodendrocytes.

GAD65-positive cells migrate from SVZ to corpus callosum

To determine the migratory potential and origin of GAD65-GFP–positive cells in demyelinated corpus callosum, we used cell transplantation of SVZ GAD65-GFP–positive cells into wild-type host SVZ, long-term BrdU retention and retroviral injection into SVZ of GAD65-GFP mice. FACS-purified GAD65-GFP–positive cells from adult SVZ were transplanted into the lateral ventricle of wild-type host brains. In NaCl-injected brains, grafted GAD65-GFP–positive cells migrated along the RMS toward the olfactory bulb (**Fig. 2a,b**). Conversely, in LPC-injected brains, grafted GAD65-GFP–positive cells were found in the RMS and olfactory bulb, and in demyelinated corpus callosum at 5 and 10 dpl, suggesting that demyelination redirected migration of some GAD65-GFP–positive progenitors toward the lesion site. These GAD65-GFP–positive cells had oligodendrocytic phenotypes (Olig2, CC1 and MBP positive, Pax6 negative; **Fig. 2c–g**).

Figure 3 Cellular characterization of the corpus callosum in Dcx-GFP mice after demyelination. (**a–j**) Images of Dcx-GFP–positive cells in the ASVZ (**a,b**) at 5 dpl and in corpus callosum (**c–j**) at 10 dpl after NaCl (**a,c,e,g,i**) and LPC (**b,d,f,h,j**) injections. Cells were labeled with antibodies to Mash1 and Olig2 (**a,b**), NG2 (**c,d**), Olig2 (**e,f**), CC1 (**g,h**) and CNP (**i,j**), together with DAPI. Insets magnify cells indicated by arrows. Dotted lines bound ASVZ and corpus callosum. Scale bars represent 50 μm. (**k**) The total number of Dcx-GFP–positive cells increased in the corpus callosum after LPC injection at 10 dpl. Bar graphs represent means ± s.e.m. ($n = 4$ brains, $*P < 0.02$, t test). (**l**) Percentages of Dcx-GFP–positive cells colabeled with antibodies to NG2, Olig2, CC1 and CNP in LPC- and NaCl-injected corpus callosum at 10 dpl. Mature oligodendrocytes stained with antibodies to CC1 and CNP were detected in corpus callosum after demyelination. Bar graphs represent means ± s.e.m. ($n = 4$ brains, $***P < 0.05$, t test).

proliferate within in callosum several days after demyelination, but originated from the SVZ and migrated to the lesion.

To confirm the origin of GAD65-GFP–positive cells in demyelinated corpus callosum, we retrovirally labeled SVZ NPCs 72 h before LPC-induced demyelination and analyzed their migration and differentiation. Consistent with transplantation and BrdU labeling results, we found a substantial number of retrovirally labeled GAD65-GFP–positive, dsRed-positive cells in demyelinated corpus callosum (7–14 dpl), indicating that GAD65-GFP–positive cells from SVZ were migrating toward corpus callosum after demyelination. GAD65-GFP–positive, dsRed-positive cells in demyelinated corpus callosum expressed oligodendrocytic markers, including Olig2, CC1 and S100β (**Supplementary Fig. 4**). These GAD65-GFP–positive, dsRed-positive cells did not express GFAP (data not shown). In NaCl-injected brains, GAD65-GFP–positive, dsRed-positive cells were not observed in corpus callosum, but were present in olfactory bulb (data not shown). These results indicate that GAD65-GFP–positive cells in demyelinated corpus callosum originated in and migrated from the SVZ.

Dcx+ cells generate oligodendrocytes after demyelination

To ascertain whether demyelination induces cell lineage plasticity in neuroblasts, we induced focal demyelination in adult corpus callosum of Dcx-GFP transgenic mice. In these mice, Dcx-GFP–positive cells are neuroblasts, as Dcx is expressed in cells committed to a neuronal lineage[20]. We found a dense population of Dcx-GFP–positive cells in the SVZ of adult Dcx-GFP mice (**Fig. 3**). In the SVZ of NaCl-injected mice, none of the Dcx-GFP–positive cells expressed Mash1 or Olig2 (**Fig. 3a**), but a substantial percentage of Dcx-GFP–positive cells in the SVZ expressed Mash1 and Olig2 after LPC injection (**Fig. 3b**). The percentage of proliferating Dcx-GFP–positive cells in SVZ was unchanged after LPC injection, compared with NaCl-injected corpus callosum (LPC = 2.72 ± 0.34%, NaCl = 2.93 ± 0.36%). In NaCl-injected corpus callosum, we found a few Dcx-GFP–positive, Dcx-GFP–positive and NG2-positive, and Dcx-GFP–positive and Olig2-positive cells (**Fig. 3c,e,k,l**); after focal demyelination, the numbers of cells with these phenotypes increased markedly (**Fig. 3d,f,k,l**). At 5 dpl, 8.43 ± 2.93% of Dcx-GFP–positive, Olig2-positive cells also expressed Dcx ($n = 3$; data not shown). Finally, in demyelinated corpus callosum, but not in NaCl-injected brains, Dcx-GFP–positive cells also expressed the mature oligodendrocyte markers CC1 and CNP (**Fig. 3g–j,l**). Together, these results from two strains of mice (GAD65-GFP and Dcx-GFP) suggest that pathological demyelination induces an increase in neuroblast-generated oligodendrocytes in demyelinated lesions.

To determine whether neuroblasts generate oligodendrocytes after demyelination, we performed LPC injections in Dcx-CreER[T2] transgenic mice (see Online Methods) and characterized the progeny of

In birth-dating experiments of GAD65-GFP–positive cell progenies, we injected BrdU every 24 h for 5 consecutive days after NaCl or LPC injections. Immunohistochemical analysis carried out 2 d after BrdU injections (7 dpl) revealed that 66.7 ± 3.7% of GAD65-GFP–positive cells in demyelinated corpus callosum were BrdU positive and expressed the oligodendrocytic markers Olig2 and CC1, but not GFAP (**Supplementary Fig. 3**). We BrdU pulse-labeled GAD65-GFP–positive cells for 2 h at 5 and 10 dpl and found no GAD65-GFP– and BrdU-positive cells in corpus callosum (data not shown), indicating that GAD65-GFP–positive cells did not
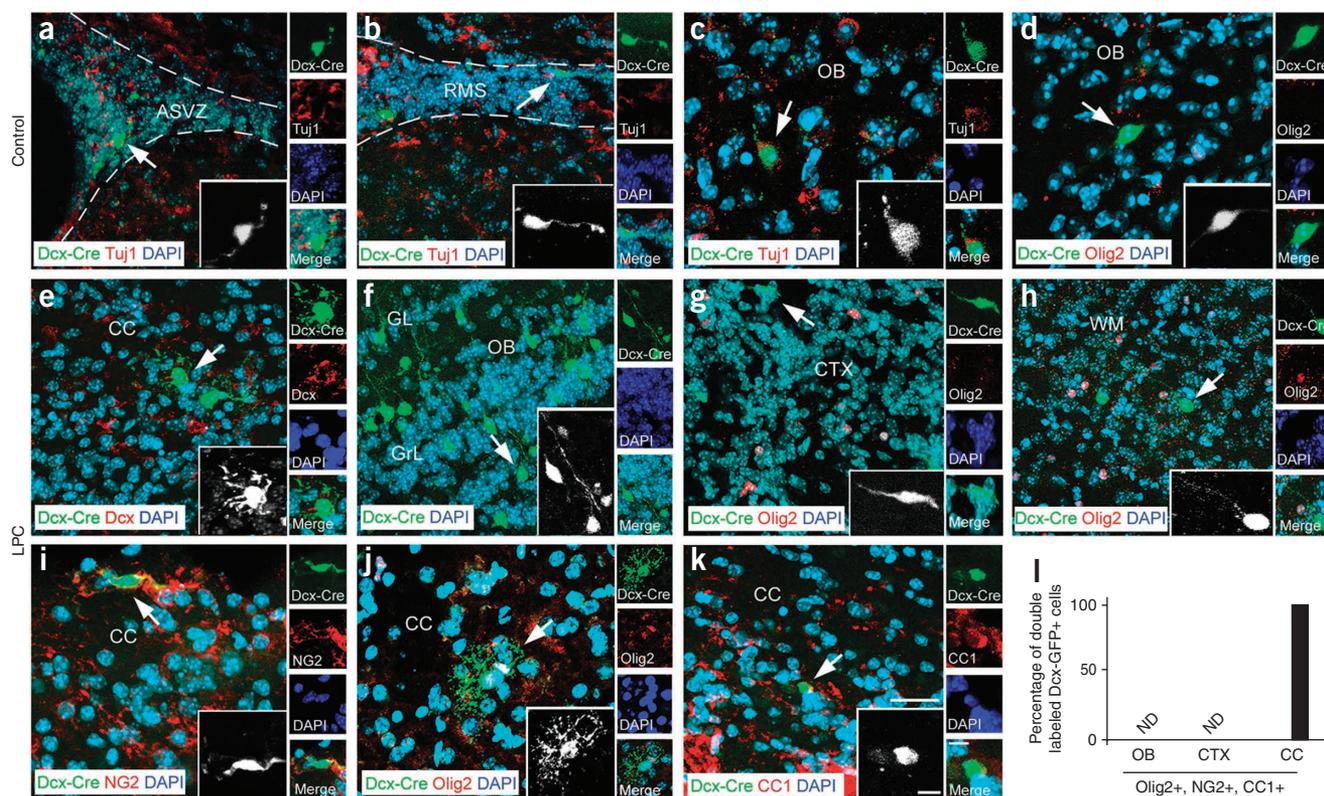
Figure 4 Cell lineage plasticity of Dcx-expressing progenitors after demyelination. (**a–k**) Confocal images of ASVZ (**a,e**), RMS (**b**), olfactory bulb (**c,d,f**), cortex (**g**), white matter (WM, **h**) and CC (**i–k**) from NaCl- (**a–d**) and LPC-injected (**e–k**) Dcx-CreER^{T2} brains at 7 dpl. Tissue sections were stained with antibodies to Tuj1 (**a–c**), Dcx (**e**), Olig2 (**d,g,h,j**), NG2 (**i**) and CC1 (**k**). In the Dcx-CreER^{T2} mouse, all of the Dcx-CreER^{T2}–GFP–positive cells had neuronal bipolar morphology and expressed the Tuj1 neuronal marker 2 d after tamoxifen injection. In LPC-injected Dcx-CreER^{T2} brains, Dcx-CreER^{T2}–GFP–positive cells had neuronal morphology in cortex, olfactory bulb and white matter, whereas Dcx-CreER^{T2}–GFP–positive cells had oligodendrocyte morphology and expressed oligodendrocyte markers in corpus callosum. Scale bars represent 200 μm (**a,b**), 100 μm (**c–k**) and 50 μm (insets). Black and white insets magnify cells indicated by arrows. (**l**) Graph represents the percentage of Dcx-CreER^{T2}–GFP–positive cells expressing Olig2, NG2 or CC1 in the olfactory bulb, cortex and corpus callosum. No oligodendrocyte lineage cells were found in the olfactory bulb and cortex, whereas in corpus callosum all Dcx-CreER^{T2}–GFP–positive cells expressed oligodendrocyte markers. The bar graph shows means ± s.e.m. ($n = 3$ brains for each, NaCl and LPC injection, ***$P < 0.05$, t test).

Dcx-CreER^{T2}–derived cells. In adult SVZ, 2 d after tamoxifen injection, Dcx-CreER^{T2}–GFP–positive cells in the SVZ, RMS and olfactory bulb had neuronal morphologies and expressed the neuronal marker βIII tubulin (Tuj1). These cells did not express Olig2 (**Fig. 4a–d**). To increase targeting of large numbers of Dcx-CreER^{T2}–GFP–positive cells in LPC-injected brains, we injected tamoxifen intraperitonally 24 h before and 24 h after LPC injections. At 14 dpl, the majority of GFP-positive cells in the olfactory bulb and cortex had mature neuronal morphologies and all of them expressed neuronal markers, including Tuj1, MAP2 and NeuN (data not shown). Notably, demyelinated lesions contained no cells with neuronal morphology, but many GFP-positive cells had oligodendrocyte morphologies. All corpus callosum cells expressed oligodendrocyte markers, including NG2, Olig2, CC1 and CNP (**Fig. 4e–l**).

Chordin promotes oligodendrogenesis from SVZ cells *in vitro*
To further examine neuronal progenitor cell lineage plasticity after demyelination, we FACS purified and cultured GAD65-GFP–positive cells from the SVZ of LPC- and NaCl-injected brains and analyzed their differentiation potential *in vitro* (**Fig. 5a**). In cultures from NaCl-injected brains, all GAD65-GFP–positive cells expressed MAP2; no GAD65-GFP–positive, Olig2-posiive and GAD65-GFP–positive, GalC-positive cells were present, confirming their neuronal phenotype (**Fig. 5b,c**). In cultures from

LPC-injected brains, a significant percentage of GAD65-GFP–positive cells had an oligodendrocyte morphology and expressed Olig2 and GalC ($P < 0.05$; **Fig. 5a–c**). These cultures had a significantly higher percentage of GAD65-GFP–positive, Mash1-positive cells and a lower percentage of GAD65-GFP–positive, MAP2-positive cells than did cultures from NaCl-injected brains ($P < 0.05$ and $P < 0.03$, respectively; **Fig. 5c**).

To identify the cellular signal promoting cell lineage plasticity of GAD65-GFP–positive and Dcx-GFP–positive progenitors, we performed microarray analysis on SVZ tissue 5 dpl from LPC- and NaCl-injected brains. Demyelination induced expression of *Crhr2*, *Cx3cr1*, *Il10r*, *Stat3*, *Tgfb1* and *Vegf*, among other genes. Using RT-PCR in SVZ from LPC-injected tissue, we found changes in the expression of BMP pathway elements, including increased *Chrd*, *Nog* and *ChorR*, and decreased *Bmp4*, compared with NaCl-injected tissue (**Supplementary Fig. 5**). Selecting vascular endothelial growth factor (VEGF) and chordin as candidates that might alter the lineage potential of GAD65-GFP–positive cells, we tested their activity in FACS-purified GAD65-GFP–positive cells from SVZ cultured in basal conditions. Neither VEGF nor chordin expanded or promoted proliferation of the GAD65-GFP–positive cell population. However, the number of GAD65-GFP–positive cells expressing Mash1, Olig2 or GFAP increased significantly in the presence of chordin, as compared with cells cultured under VEGF or control conditions
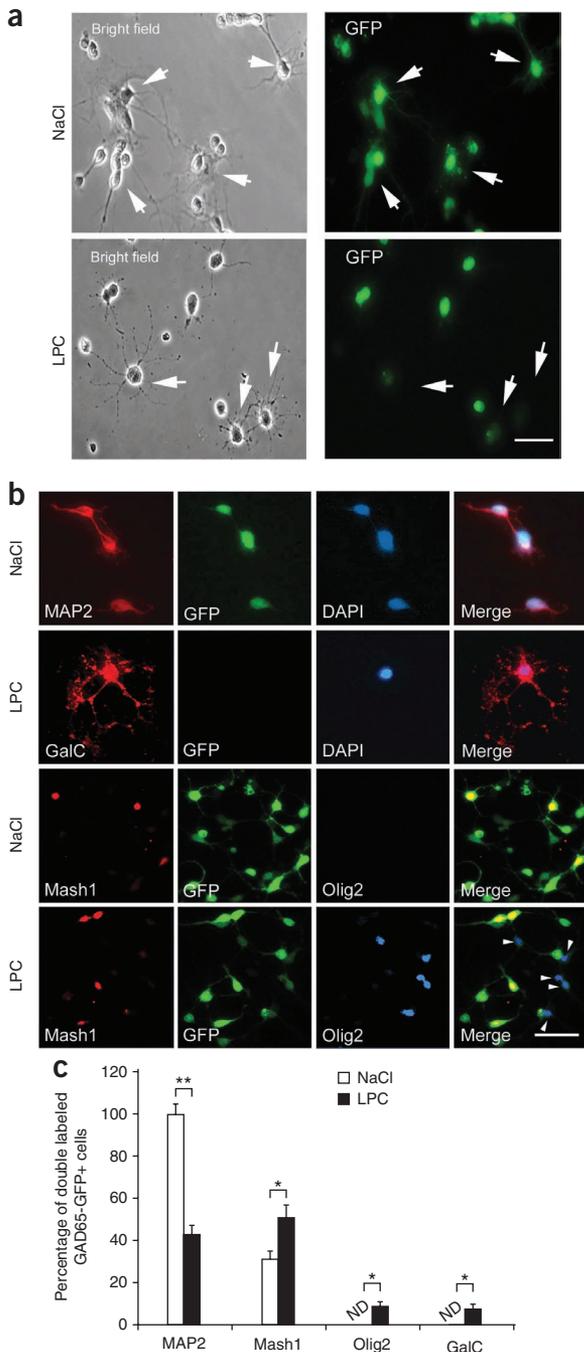
Figure 5 GAD65-GFP–positive cells from the SVZ of LPC-injected brains generate Olig2- and GalC-positive cells in culture. (**a**) Bright field (left) and fluorescence (right) images of cultured FACS-purified SVZ GAD65-GFP–positive cells from NaCl- or LPC-injected brains. Arrows indicate GAD65-GFP–positive cells with neuronal (cultures from NaCl-injected brains) or oligodendrocytic (cultures from LPC-injected brains) morphologies. Scale bar represents 50 μm. (**b**) Images of FACS-purified SVZ GAD65-GFP–positive cells from NaCl- and LPC-injected brains cultured for 5 d and immunostained with antibodies to MAP2, GalC, Mash1 or Olig2. Scale bar represents 30 μm. (**c**) Percentages of GAD65-GFP–positive cells expressing MAP2, Mash1, Olig2 and GalC in 5-d cultures obtained from SVZ cells of NaCl- or LPC-injected brains. Cultures from NaCl-injected brains consisted of 100% MAP2-positive cells; no Olig2- or GalC-positive cells were detected. A percentage of MAP2-positive cells coexpressed Mash1. Cultures from LPC-injected brains consisted of GAD65-GFP–positive, Olig2-positive cells and GAD65-GFP–positive, GalC-positive cells. Bar graphs represent means ± s.e.m. (n = 3 independent cultures, *P < 0.05, **P < 0.03, t test).

with or without chordin. At 24 h in culture, virtually all (99.1 ± 0.96%) Dcx-GFP–positive cells expressed MAP2; a small percentage was Olig2 positive (0.9 ± 0.05%; **Supplementary Fig. 6**). After 5 d *in vitro*, control cultures consisted mainly of neurons (68.5 ± 0.5%) and a small percentage of oligodendrocytes (0.7 ± 0.01%). Conversely, cells cultured with chordin had a greater percentage of GalC–positive cells (**Fig. 7b,d,e**). Similar to GAD65-GFP–positive cell cultures, the percentage of Dcx-GFP–positive, Ki67-positive cells in the presence of chordin did not change compared to cells cultured in basal medium (chordin = 4.69 ± 1.55%, basal medium = 4.06 ± 0.2). Using RT-PCR, we found elevated levels of *Olig2* and *Mbp* mRNAs in Dcx-GFP–positive cells after chordin treatment compared with basal conditions; treatment with antibody to chordin blocked this effect. Neither control cultures nor chordin treatment elicited changes in the percentage of GFAP-positive cells or in *Gfap* mRNA expression (**Fig. 7**). Altogether, these results from GAD65-GFP–positive and Dcx-GFP–positive cell cultures indicate that chordin influences the differentiation potential of GAD65- and Dcx-expressing cells by promoting oligodendrogenesis.

Chordin promotes oligodendrogenesis from SVZ cells *in vivo*

To study chordin involvement in GAD65-GFP–positive progenitor cell lineage plasticity after demyelination *in vivo*, we implanted Alzet minipumps releasing saline, chordin or antibody to chordin in SVZ of LPC- or NaCl-injected brains (**Fig. 8**). Infusing antibody to chordin after LPC-induced demyelination decreased the number of GAD65-GFP–positive cells (**Fig. 8e**) and the percentage of GAD65-GFP–positive cells expressing Mash1, Olig2 and CC1 in the lesion area, as compared with saline infusion (**Fig. 8c,f**). Infusing chordin increased the number of GAD65-GFP–positive cells (**Fig. 8e**) and of GAD65-GFP–positive cells expressing Mash1, Olig2, CC1 and GFAP in the lesion area (**Fig. 8a,f**), as compared with saline infusion. Consistent with our *in vitro* findings, a large percentage of GAD65-GFP–positive, GFAP-positive cells were detected after chordin infusion (**Fig. 8f**). These cells did not coexpress Olig2 or Mash1 (data not shown).

In NaCl-injected corpus callosum, chordin infusion significantly increased the number of GAD65-GFP–positive cells in corpus callosum compared with saline infusion (**Fig. 8g**); antibody to chordin had no effect alone (**Fig. 8b,d,g**). In these experiments, GAD65-GFP–positive cells in corpus callosum expressed Mash1, Olig2, GFAP and CC1 after chordin infusion, but no double-positive cells were detected after saline or antibody to chordin infusion (**Fig. 8f**). These results, and the *in vitro* assay, indicate that chordin induces Mash1

(P < 0.03). Cultures in basal medium and with VEGF contained mostly neurons, as shown by MAP2 immunolabeling (**Fig. 6a–f**). RT-PCR analysis revealed that *Olig2* and *Mash1* were not prominently expressed in control and VEGF-treated cultures, but chordin exposure enhanced their expression (data not shown). To examine chordin's influence on GAD65-GFP–positive cell lineage potential, we FACS purified cells from the SVZ of normal brains and cultured them with chordin and with antibody to chordin. Antibody to chordin prevented glial differentiation of GAD65-GFP–positive progenitors in culture, as seen by a reduced percentage of GAD65-GFP–positive, Olig2-positive and GAD65-GFP–positive, Mash1-positive cells and downregulation of oligodendrocyte gene expression (**Fig. 6g–i**).

We FACS purified Dcx-GFP–positive cells from the SVZ of Dcx-GFP mice after LPC-induced demyelination and cultured them
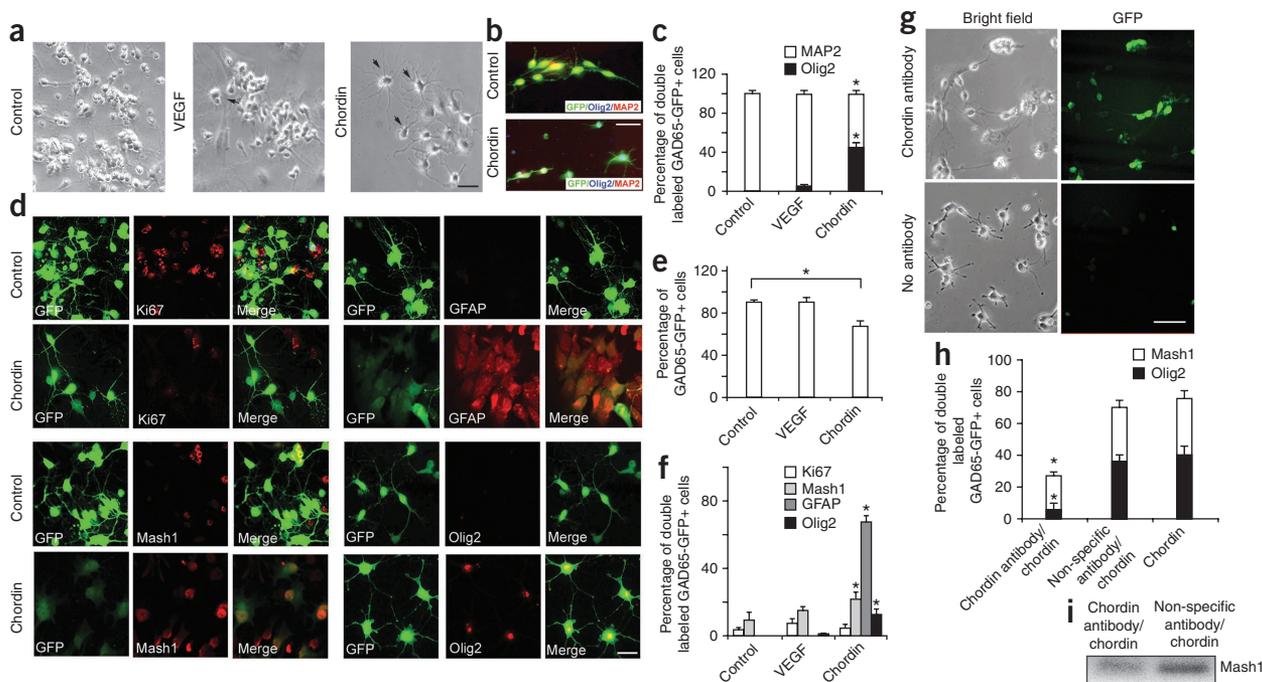
Figure 6 Chordin induces cell lineage plasticity in cultured SVZ GAD65-GFP–positive cells. Cultures were processed at 5 d. (**a**) FACS-sorted SVZ GAD65-GFP–positive cells cultured in basal medium and with VEGF or chordin. Arrows indicate oligodendrocytes. Scale bar represents 20 µm. (**b**) GAD65-GFP–positive cells immunostained with antibodies to Olig2 and MAP2. Scale bar represents 20 µm. (**c**) Percentages of GAD65-GFP–positive, MAP2-positive cells and GAD65-GFP–positive, Olig2-positive cells in designated cultures. Bar graphs represent means ± s.e.m. ($n = 3$ independent cultures,*$P < 0.05$, t test). (**d**) FACS-sorted SVZ GAD65-GFP–positive cells cultured in basal medium with or without chordin. GAD65-GFP–positive cells immunostained with antibodies to Ki67, Mash1, GFAP or Olig2. Scale bar represents 20 µm. (**e**) Percentages of total GAD65-GFP–positive cells under different culture conditions. Means ± s.e.m. are shown ($n = 3$ independent cultures, *$P < 0.05$, t test). (**f**) Percentages of total GAD65-GFP–positive cells that express Ki67, Mash1, GFAP or Olig2 in basal medium in the presence of VEGF or chordin. Means ± s.e.m. are shown ($n = 3$ independent cultures, **$P < 0.03$, t test). (**g**) FACS-purified SVZ GAD65-GFP–positive cells cultured with chordin and either antibody to chordin or with a nonspecific IgG antibody. Scale bar represents 40 µm. (**h**) Percentages of GAD65-GFP–positive, Mash1-positive cells and GAD65-GFP–positive, Olig2-positive cells in chordin-treated cultures compared with cells cultured with nonspecific antibody and chordin or chordin alone. Means ± s.e.m. are shown ($n = 3$ independent cultures, t test). (**i**) RT-PCR from FACS-purified SVZ GAD65-GFP–positive cells maintained in culture in the presence of chordin.

and Olig2 expression in SVZ GAD65-GFP–positive cells, regulating their lineage potential after demyelination.

To confirm that chordin changes the *in vivo* lineage potential of neuroblasts after demyelination, we implanted chordin minipumps in Dcx-GFP mice. In demyelinated corpus callosum, we found no difference between saline and chordin infusion in the total number of Dcx-GFP–positive cells. However, in NaCl-injected brains, chordin infusion caused a fivefold increase in the number of Dcx-GFP–positive cells (**Fig. 8l**). In NaCl-injected brains, chordin infusion increased the percentage of Dcx-GFP–positive cells coexpressing NG2, Olig2, CC1 and CNP; these cell types were not present after NaCl infusion (**Fig. 8n**). Conversely, in LPC brains, chordin significantly increased the percentage of progenitors expressing NG2 and Olig2, as well as CC1- and CNP-expressing mature oligodendrocytes, as compared with saline infusion ($P < 0.05$; **Fig. 8h–k,m**). In LPC-injected brains, the number of astrocytes was low and was not substantially modified by chordin infusion (**Fig. 8m**). Thus, our *in vivo* results confirmed that chordin infusion in demyelinated corpus callosum regulates the cell lineage potential of neuroblasts to promote oligodendrogenesis.

DISCUSSION
Using several transgenic mouse strains, we examined whether endogenous adult SVZ NPCs have lineage plasticity under pathological conditions. We found that GAD65- and Dcx-expressing NPCs, which

normally generate neurons, produced oligodendrocytes in corpus callosum after demyelination. Chordin expression was enhanced in SVZ after demyelination, and this BMP antagonist induced lineage plasticity of GAD65- and Dcx-expressing NPCs.

NPC lineage plasticity after demyelination
Several studies have found that demyelination causes cellular responses in different NPC pools of adult brain. In various animal models of demyelination, enhanced proliferation occurs in cells with the oligodendrocyte progenitor cell (OPC) phenotype, expressing NG2, PDGFRα, Olig2 and Mash1 (refs. 13,14,21). A local endogenous pool of OPCs is apparently involved in repopulating and remyelinating demyelinated lesions[14,22,23]; however, SVZ progenitors with an OPC phenotype also proliferate and migrate to areas of demyelination to generate remyelinating oligodendrocytes[11,14]. Notably, both pools of OPCs are found in the brain tissue of individuals with multiple sclerosis, either in or near demyelinating lesions and in SVZ[15,23,24]. These progenitors express NG2, PDGRα and Olig2, and additional oligodendrocyte markers, including Sox9 and Sox10 (refs. 15,23,24).

Contrasting with previous findings in different NPC types[11,14,22,23], our results indicate that oligodendrocytes can be generated in the absence of cell proliferation from a subset of adult SVZ progenitors after demyelination. *In vivo* analysis revealed that neither the proliferation index nor cell number of GAD65-GFP–positive NPCs of
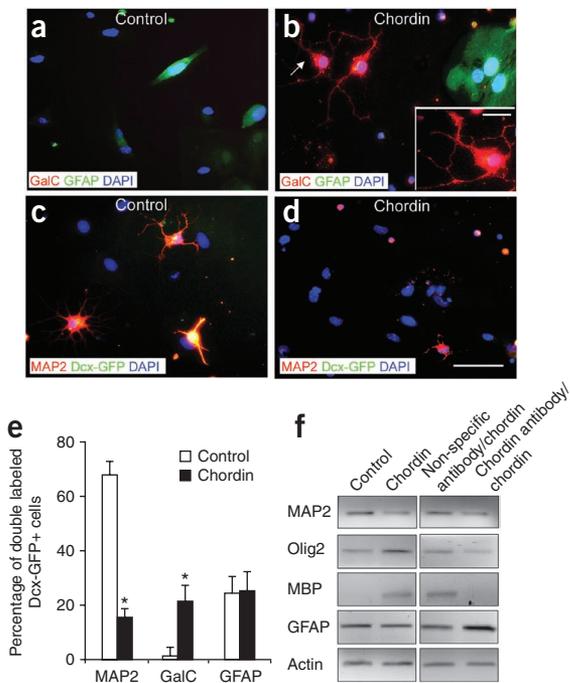
Figure 7 Chordin induces cell lineage plasticity in cultured SVZ Dcx-GFP–positive cells. (a–d) Dcx-GFP–positive cells FACS purified from the adult SVZ were cultured for 5 d in basal medium (a,c) and in medium with chordin and antibody to chordin (b,d). Cells were stained with anti-GFAP, anti-GalC and anti-MAP2 antibodies. Scale bars represent 20 μm and 50 μm (inset). Inset magnifies oligodendrocyte indicated by arrow. (e) Chordin decreased the percentage of Dcx-GFP–positive cells expressing MAP2 and increased the percentage of Dcx-GFP–positive, GalC-positive cells in the cultures. The percentage of Dcx-GFP–positive, GFAP-positive astrocytes remained unchanged. Bar graphs represent means ± s.e.m. (n = 3 independent cultures, $*P < 0.05$, t test). (f) RT-PCR from Dcx-GFP–positive cells FACS purified from the adult SVZ and cultured for 5 d. Upregulation of *Olig2* and *Mbp* expression was detected after treatment with chordin. No substantial changes were observed in *Gfap* expression. Treatment with antibody to chordin downregulates *Olig2* and *Mbp* genes.

SVZ changed after demyelination, although these cells produced oligodendrocytes in corpus callosum. Analysis in cell cultures indicated that chordin did not increase GAD65-GFP–positive cell proliferation or number. We conclude that more oligodendrocytes are generated from GAD65-GFP–positive progenitors as a result of enhanced differentiation, rather than expansion of a subset of oligodendrocyte-committed progenitors. In Dcx-GFP mice, there was a lack of Dcx-GFP–positive cell proliferation after demyelination *in vivo* and after treatment with chordin in culture, supporting these conclusions. Overall, our results indicate that demyelination and chordin directly affect GAD65- and Dcx-expressing NPC cell differentiation, rather than proliferation.

It is not known whether different SVZ NPC populations, including neuroblasts, are exclusively committed to neuronal or glial fates in adult brain under physiological or pathological conditions. Overexpression of Pax6 in astrocytes induces neurogenesis[25] and Cdk2 overexpression in SVZ progenitors induces expression of bHLH transcription factor Olig2 and enhances oligodendrogenesis[26]. Acute and chronic brain injuries cause Olig2 upregulation in injured parenchyma, while generating oligodendrocytes and astrocytes[19]. In the same pathological models, Olig2 loss of function results in neuron generation[19]. Another study found that cortical lesions caused transient changes in migration patterns of SVZ progeny[27]. Migration to olfactory bulb was reduced, but migration toward the injury and differentiation along glial lineages were enhanced[27].

Our results support that, under pathological conditions, cell lineage plasticity is induced in a subpopulation of NPCs that are normally committed to neuronal fates. We found that oligodendrocytes were generated from GAD65- and Dcx-expressing NPCs of adult SVZ of three different mouse strains, including a Dcx-CreER[T2] mouse that allows direct cell-fate mapping after focal demyelination of corpus callosum. In all of the mouse strains analyzed, GAD65- and Dcx-derived cells at different stages of oligodendrocyte lineage are found in corpus callosum after demyelination, indicating that mature CC1-, CNP- and MBP-positive oligodendrocytes are derived from cells that develop progressively from progenitors to myelinating cells. Consistent findings from all mouse strains suggest that chordin promotes oligodendrogenesis from GAD65- and Dcx-expressing NPCs, *in vitro* and *in vivo*,

in response to demyelination. Although other signals are upregulated in SVZ after demyelination, our results with antibody to chordin *in vivo* indicate that chordin is important for the lineage plasticity of GAD65- and Dcx-expressing NPCs; selective antibodies prevented its effects on oligodendrogenesis after focal demyelination.
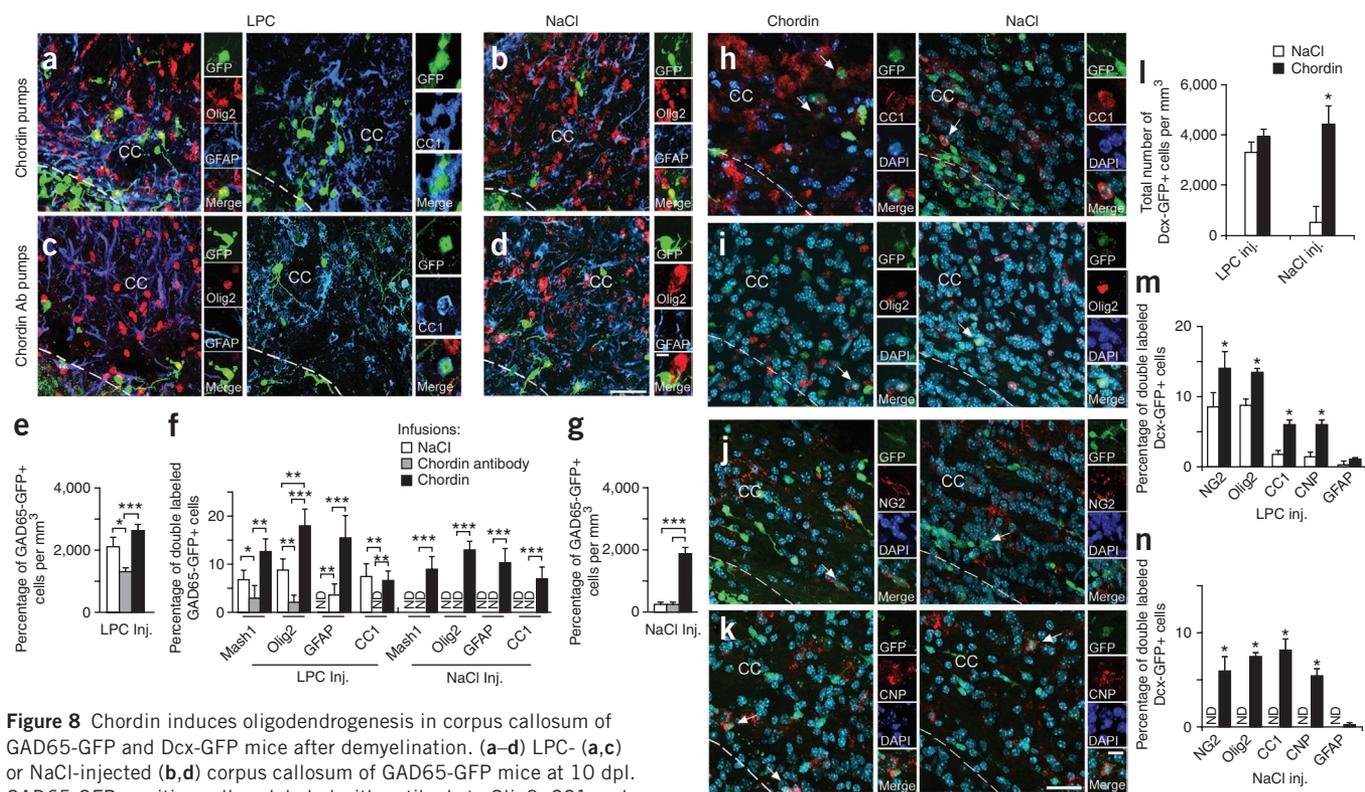
A recent study found that, under normal physiological conditions, retrovirus-mediated overexpression of Mash1 in adult hippocampal progenitor cells redirected their fate to generate oligodendrocytes[18]. We found this process in a different NPC population following corpus callosum demyelination without molecular manipulation of GAD65- and Dcx-expressing NPCs. Cell lineage plasticity in these NPCs accompanied expression of both Mash1 and Olig2, suggesting that these bHLH transcription factors are coordinated as essential regulators of oligodendrogenesis from GAD65- and Dcx-expressing NPCs.

Chordin regulates oligodendrogenesis after demyelination

We found that focal demyelination causes upregulation of several putative signals in SVZ, including epidermal growth factor receptor (EGFR) ligands[14]. Our analyses suggest a functional role for EGFR activity in OPC proliferation in SVZ and migration from SVZ to demyelinated areas of corpus callosum[14]. We found that EGFR activity is involved in promoting developmental myelination and oligodendrocyte repair and remyelination from SVZ OPCs after focal demyelination[14]. Our results suggest that an endogenous BMP signaling antagonist promotes SVZ NPC lineage plasticity and differentiation to generate glia after demyelination.

BMP signaling regulates various developmental processes in neural stem cells and in NPCs under normal physiological conditions[28]. In particular, BMPs have been shown to promote dorsal identity, regulate cell proliferation and induce multiple terminal fates during embryonic and postnatal development[28,29]. BMPs' developmental effects are complex, often paradoxical, and probably depend on involvement of distinct signal transduction pathways and interactions with other developmental signals[28]. BMP signaling is known to suppress oligodendrogenesis and promote astrogliogenesis[30]. BMPs negatively control OPC specification and lineage commitment[30–34], as well as OPC maturation to myelinating oligodendrocytes[30,35]. These effects likely involve suppression of Id (inhibitor of differentiation) protein expression and Olig protein regulation[28,34,36,37].

BMP expression is enhanced in different animal models of CNS disorders and injury, including ischemia, stroke, spinal cord injury and stab injury[30]. Many experimental procedures result in demyelination or impaired remyelination[28,38]. BMP-7 exerts protective and regenerative effects in stroke[28,39,40], BMP-6 reduces ischemia/reperfusion injury[36], and BMPs have a protective role in models of spinal cord injury[38] and traumatic brain injury[41,42]. In animal models

Figure 8 Chordin induces oligodendrogenesis in corpus callosum of GAD65-GFP and Dcx-GFP mice after demyelination. (**a**–**d**) LPC- (**a**,**c**) or NaCl-injected (**b**,**d**) corpus callosum of GAD65-GFP mice at 10 dpl. GAD65-GFP–positive cells colabeled with antibody to Olig2, CC1 and GFAP after chordin (**a**) or antibody to chordin (**b**) infusion. Scale bar represents 50 μm. (**e**) GAD65-GFP–positive cell numbers after NaCl, chordin and antibody to chordin infusion in LPC-injected corpus callosum. Bars represent means ± s.e.m. ($n = 4$ brains per condition, $*P < 0.05$, $***P < 0.02$, t test). (**f**) Percentages of GAD65-GFP–positive cells expressing glial markers in LPC- and NaCl-injected corpus callosum. Bars represent means ± s.e.m. ($n = 4$ brains per condition, $**P < 0.03$, t test). (**g**) GAD65-GFP–positive cell numbers after NaCl, chordin and antibody to chordin infusion in NaCl-injected corpus callosum. Bars represent means ± s.e.m. ($n = 4$ brains per condition, t test). Dcx–GFP–positive cells colabeled with antibodies to CC1 (**h**), Olig2 (**i**), NG2 (**j**) and CNP (**k**) in LPC-injected Dcx-GFP brains after chordin or NaCl infusion at 10 dpl. Scale bars represent 50 μm. (**l**) Dcx-GFP–positive cell number after NaCl and chordin infusion in corpus callosum of LPC- and NaCl-injected brains. Bars represent means ± s.e.m. ($n = 4$ brains per condition, t-test). (**m**) Percentages of Dcx-GFP–positive cells expressing NG2 or glial markers in LPC-injected brains after NaCl or chordin infusion. Bars represent means ± s.e.m. ($n = 4$ brains per condition, t test). (**n**) Percentages of Dcx-GFP–positive cells expressing NG2 or glial markers in NaCl-injected brains after NaCl or chordin infusion. Bars represent means ± s.e.m. ($n = 4$ brains per condition, t test). Dotted lines define lesion boundaries. The cells indicated arrows are magnified in insets.

of demyelination, BMP expression is upregulated in demyelinated lesions[30], BMP-4 expression is upregulated after focal demyelination[43,44], and BMP-4, BMP-6 and BMP-7 expression is enhanced in experimental immune encephalomyelitis[45]. However, unlike the protective effects observed in other CNS-injury procedures, BMPs inhibit remyelination and impair recovery[30]. These findings indicate that suppressing BMP signaling may exert opposite effects in different types of injury, likely as a result of selective effects of BMPs in distinct neural cell types and interaction between BMP-activated pathways and other cellular signals turned on under different pathological conditions.

Our findings in SVZ GAD65- and Dcx-expressing NPCs after demyelination suggest that BMPs have an inhibitory effect in oligodrogliogenesis. Pathological insult induced a molecular response in the SVZ, upregulation of the BMP antagonist chordin, that promotes oligodendrocyte production from GAD65- and Dcx-expressing progenitors. As these cells are committed neuronal progenitors under normal physiological conditions, our results suggest that BMP signaling restricts their fate to generating neurons in normal adult brain by suppressing an oligodendrocyte fate. This conclusion is supported by the recent demonstration that Smad4 deletion and Noggin infusion in adult SVZ strongly enhance migration of Olig2-expressing cells to the corpus callosum, where they differentiate into mature

oligodendrocytes[46], a process that is observed in normal brain only after molecular manipulation of BMP signaling in SVZ. Our findings on chordin-induced oligodendrogenesis from GAD65- and Dcx-expressing NPCs indicate that similar mechanisms can be activated by pathological insult, overcoming cell lineage restrictions in these NPC populations.

Strategies aimed at enhancing the generation of viable, mature oligodendrocytes from NPCs or neural stem cells will require combined cellular and molecular approaches. These include genetic manipulation of crucial molecular regulators of oligodendrocyte fate determination and identification of specific NPC populations and cellular signals promoting or preventing oligodendrogenesis from these NPCs. Our results indicate that demyelinating insult in the adult CNS produces an endogenous regenerative response in a specific population of NPCs of the adult SVZ. This response involves neutralizing BMP signaling to promote cell lineage plasticity in neuroblasts. Notably, increased interneuron production has also been demonstrated in the SVZ of multiple sclerosis tissue and at the site of multiple sclerosis lesions[47]. As BMP expression is enhanced in multiple sclerosis plaques[48], our findings identify specific cellular and molecular targets with the potential to enhance oligodendrocyte regeneration from endogenous NPCs under pathological conditions affecting myelin.

ARTICLES

METHODS

Methods and any associated references are available in the online version of the paper at http://www.nature.com/natureneuroscience/.

Accession codes. Microarray data have been deposited in the Gene Expression Omnibus under accession code GSE21310.

Note: Supplementary information is available on the Nature Neuroscience website.

AUTHOR CONTRIBUTIONS

B.J. and A.A. designed, performed and analyzed all of the experiments. M.R. performed some of the *in vivo* experiments, cell imaging and cell counting. G.S. generated and provided the GAD65-GFP mice. Y.K., K.A.S., G.M. and H.S. generated and provided the Dcx-CreER^T2 mice. V.G. designed the experiments with B.J. and A.A., supervised the project and wrote the manuscript with input from B.J.

COMPETING FINANCIAL INTERESTS

The authors declare no competing financial interests.

Published online at http://www.nature.com/natureneuroscience/.
Reprints and permissions information is available online at http://www.nature.com/reprintsandpermissions/.

1. Doetsch, F., Garcia-Verdugo, J.M. & Alvarez-Buylla, A. Regeneration of a germinal layer in the adult mammalian brain. *Proc. Natl. Acad. Sci. USA* **96**, 11619–11624 (1999).
2. Palmer, T.D., Markakis, E.A., Willhoite, A.R., Safar, F. & Gage, F.H. Fibroblast growth factor 2 activates a latent neurogenic program in neural stem cells from diverse regions of the adult CNS. *J. Neurosci.* **19**, 8487–8497 (1999).
3. Palmer, T.D., Willhoite, A.R. & Gage, F.H. Vascular niche for adult hippocampal neurogenesis. *J. Comp. Neurol.* **425**, 479–494 (2000).
4. Temple, S. The development of neural stem cells. *Nature* **414**, 112–117 (2001).
5. Shen, Q., Zhong, W., Jan, Y.N. & Temple, S. Asymmetric Numb distribution is critical for asymmetric cell division of mouse cerebral cortical stem cells and neuroblasts. *Development* **129**, 4843–4853 (2002).
6. Alvarez-Buylla, A. & Garcia-Verdugo, J.M. Neurogenesis in adult subventricular zone. *J. Neurosci.* **22**, 629–634 (2002).
7. Alvarez-Buylla, A. & Lim, D.A. For the long run: maintaining germinal niches in the adult brain. *Neuron* **41**, 683–686 (2004).
8. Coskun, V. & Luskin, M.B. Intrinsic and extrinsic regulation of the proliferation and differentiation of cells in the rodent rostral migratory stream. *J. Neurosci. Res.* **69**, 795–802 (2002).
9. Hack, M.A. *et al.* Neuronal fate determinants of adult olfactory bulb neurogenesis. *Nat. Neurosci.* **8**, 865–872 (2005).
10. Kim, Y., Comte, I., Szabo, G., Hockberger, P. & Szele, F.G. Adult mouse subventricular zone stem and progenitor cells are sessile and epidermal growth factor receptor negatively regulates neuroblast migration. *PLoS One* **4**, e8122 (2009).
11. Nait-Oumesmar, B. *et al.* Progenitor cells of the adult mouse subventricular zone proliferate, migrate and differentiate into oligodendrocytes after demyelination. *Eur. J. Neurosci.* **11**, 4357–4366 (1999).
12. Ligon, K.L. *et al.* Development of NG2 neural progenitor cells requires *Olig* gene function. *Proc. Natl. Acad. Sci. USA* **103**, 7853–7858 (2006).
13. Menn, B. *et al.* Origin of oligodendrocytes in the subventricular zone of the adult brain. *J. Neurosci.* **26**, 7907–7918 (2006).
14. Aguirre, A., Dupree, J., Mangin, J.M. & Gallo, V. A functional role for EGFR signaling in myelination and remyelination. *Nat. Neurosci.* **10**, 990–1002 (2007).
15. Nait-Oumesmar, B., Picard-Riéra, N., Kerninon, C. & Baron-Van Evercooren, A. The role of SVZ-derived neural precursors in demyelinating diseases: From animal models to multiple sclerosis. *J. Neurol. Sci.* **265**, 26–31 (2008).
16. Baumann, N. & Pham-Dinh, D. Biology of oligodendrocytes and myelin in the mammalian central nervous system. *Physiol. Rev.* **81**, 871–927 (2001).
17. Levine, J.M., Reynolds, R. & Fawcett, J.W. The oligodendrocyte precursor cell in health and disease. *Trends Neurosci.* **24**, 39–47 (2001).
18. Jessberger, S., Toni, N., Clemenson, G.D. Jr., Ray, J. & Gage, F.H. Directed differentiation of hippocampal stem/progenitor cells in the adult brain. *Nat. Neurosci.* **11**, 888–893 (2008).
19. Buffo, A. *et al.* Expression pattern of the transcription factor Olig2 in response to brain injuries: implications for neuronal repair. *Proc. Natl. Acad. Sci. USA* **102**, 18183–18188 (2005).
20. Walker, T.L., Yasuda, T., Adams, D.J. & Bartlett, P.F. The doublecortin-expressing population in the developing and adult brain contains multipotential precursors in addition to neuronal-lineage cells. *J. Neurosci.* **27**, 3734–3742 (2007).
21. Ligon, K.L., Fancy, S.P., Franklin, R.J. & Rowitch, D.H. *Olig* gene function in CNS development and disease. *Glia* **54**, 1–10 (2006).
22. Canoll, P. & Goldman, J. The interface between glial progenitors and gliomas. *Acta Neuropathol.* **116**, 465–477 (2008).
23. Franklin, R.J. & Ffrench-Constant, C. Remyelination in the CNS: from biology to therapy. *Nat. Rev. Neurosci.* **9**, 839–855 (2008).
24. Staugaitis, S.M. & Trapp, B.D. NG2-positive glia in the human central nervous system. *Neuron Glia Biol.* **5**, 35–44 (2009).
25. Heins, N. *et al.* Glial cells generate neurons: the role of the transcription factor Pax6. *Nat. Neurosci.* **5**, 308–315 (2002).
26. Jablonska, B. *et al.* Cdk2 is critical for proliferation and self-renewal of neural progenitor cells in the adult subventricular zone. *J. Cell Biol.* **179**, 1231–1245 (2007).
27. Goings, G.E., Sahni, V. & Szele, F.G. Migration patterns of subventricular zone cells in adult mice change after cerebral cortex injury. *Brain Res.* **996**, 213–226 (2004).
28. Chen, H.L. & Panchision, D.M. Concise review: bone morphogenetic protein pleiotropism in neural stem cells and their derivatives–alternative pathways, convergent signals. *Stem Cells* **25**, 63–68 (2007).
29. Schuurmans, C. & Guillemot, F. Molecular mechanisms underlying cell fate specification in the developing telencephalon. *Curr. Opin. Neurobiol.* **12**, 26–34 (2002).
30. See, J.M.P. & Grinspan, J.B.P. Sending mixed signals: bone morphogenetic protein in myelination and demyelination. *J. Neuropathol. Exp. Neurol.* **68**, 595–604 (2009).
31. Mehler, M.F., Mabie, P.C., Zhu, G., Gokhan, S. & Kessler, J.A. Developmental changes in progenitor cell responsiveness to bone morphogenetic proteins differentially modulate progressive CNS lineage fate. *Dev. Neurosci.* **22**, 74–85 (2000).
32. Mekki-Dauriac, S., Agius, E., Kan, P. & Cochard, P. Bone morphogenetic proteins negatively control oligodendrocyte precursor specification in the chick spinal cord. *Development* **129**, 5117–5130 (2002).
33. Gomes, W.A., Mehler, M.F. & Kessler, J.A. Transgenic overexpression of BMP4 increases astroglial and decreases oligodendroglial lineage commitment. *Dev. Biol.* **255**, 164–177 (2003).
34. Samanta, J. *et al.* BMPR1a Signaling determines numbers of oligodendrocytes and Calbindin-expressing interneurons in the cortex. *J. Neurosci.* **27**, 7397–7407 (2007).
35. See, J. *et al.* BMP signaling mutant mice exhibit glial cell maturation defects. *Mol. Cell. Neurosci.* **35**, 171–182 (2007).
36. Wang, Y. *et al.* Bone morphogenetic protein–6 reduces ischemia-induced brain damage in rats. *Stroke* **32**, 2170–2178 (2001).
37. Kondo, T. Common mechanism underlying oligodendrocyte development and oligodendrogliomagenesis. *Brain Nerve* **61**, 741–751 (2009).
38. Hampton, D.W. *et al.* A potential role for bone morphogenetic protein signalling in glial cell fate determination following adult central nervous system injury *in vivo*. *Eur. J. Neurosci.* **26**, 3024–3035 (2007).
39. Chou, J. *et al.* Neuroregenerative effects of BMP7 after stroke in rats. *J. Neurol. Sci.* **240**, 21–29 (2006).
40. Shen, H., Luo, Y., Kuo, C.-C. & Wang, Y. BMP7 reduces synergistic injury induced by methamphetamine and ischemia in mouse brain. *Neurosci. Lett.* **442**, 15–18 (2008).
41. Israelsson, C. *et al.* Genetically modified bone morphogenetic protein signaling alters traumatic brain injury-induced gene expression responses in the adult mouse. *J. Neurosci. Res.* **84**, 47–57 (2006).
42. Bani-Yaghoub, M. *et al.* Neuroregenerative strategies in the brain: emerging significance of bone morphogenetic protein 7 (BMP7). *Biochem. Cell Biol.* **86**, 361–369 (2008).
43. Zhao, C., Fancy, S.P.J., Kotter, M.R., Li, W.-W. & Franklin, R.J.M. Mechanisms of CNS remyelination—the key to therapeutic advances. *J. Neurol. Sci.* **233**, 87–91 (2005).
44. Fuller, M.L. *et al.* Bone morphogenetic proteins promote gliosis in demyelinating spinal cord lesions. *Ann. Neurol.* **62**, 288–300 (2007).
45. Ara, J. *et al.* Bone morphogenetic proteins 4, 6 and 7 are up-regulated in mouse spinal cord during experimental autoimmune encephalomyelitis. *J. Neurosci. Res.* **86**, 125–135 (2008).
46. Colak, D. *et al.* Adult neurogenesis requires Smad4-mediated bone morphogenic protein signaling in stem cells. *J. Neurosci.* **28**, 434–446 (2008).
47. Chang, A. *et al.* Neurogenesis in the chronic lesions of multiple sclerosis. *Brain* **131**, 2366–2375 (2008).
48. Deininger, M., Meyermann, R. & Schluesener, H. Detection of two transforming growth factor-beta-related morphogens, bone morphogenetic proteins-4 and -5, in RNA of multiple sclerosis and Creutzfeldt-Jakob disease lesions. *Acta Neuropathol.* **90**, 76–79 (1995).

ONLINE METHODS

Animals and surgical procedures. GAD65-GFP (generated by G. Szabo, Institute of Experimental Medicine) and Dcx-GFP (cat. # 000244-Mu, Jackson Laboratory) mouse colonies were maintained in the animal facility of Children's National Medical Center according to guidelines set by the Institutional Animal Care and Use Committee of the Children's National Medical Center and the US National Institutes of Health. Dcx-BAC-CreER[T2] transgenic mice were generated and maintained following procedures approved by the Animal Care and Use Committee of the Johns Hopkins University School of Medicine and the US National Institutes of Health. The mouse BAC clone RP23-462G16, containing the entire *Dcx* gene (http://bacpac.chori.org), was modified using a double homologous recombination approach with the pLD53.SC-AB shuttle vector (a kind gift of N. Heintz, Rockefeller University). The shuttle vector contains two homology regions around the *Dcx* start codon in exon2. The first homology region included the 496 base pairs between the sequence 5′-TAG CTC CCT CTG TTT CTC TTT-3′ and the reverse complement sequence 5′-ATT TTG GTG GAA CCA CAG CAA-3′. The second homology region included the 549 base pairs between the sequence 5′-GAA CTT GAT TTT GGA CAT TTT-3′ and the reverse complement sequence 5′-TTA ATT AAG GAA TGA CAG TTA-3′. A 2.0-kb fragment of pCre-ER[T2] vector (a kind gift of P. Chambon, Institut Génétique Biologie Moléculaire Cellulaire) containing the CreER[T2] cDNA and polyadenylation sequence of SV40 was inserted between the two homology regions. The shuttle vector containing the CreER[T2] insert was integrated into BAC by homologous recombination and co-integrates were identified by chloramphenicol and ampicillin selection. Resolution of co-integrates through a second homologous recombination event was achieved by negative selection on sucrose, resulting in complete excision of the shuttle vector backbone that included the *SacB* gene. The resulting modified BAC encoding *CreER[T2]* under control of the endogenous *Dcx* promoter and regulatory elements was analyzed by Southern blotting verifying proper CreER[T2] integration, sequenced over the *Dcx* gene locus and injected into mouse pronuclei. We identified 7 of 34 potential founder animals by PCR. These founders were backcrossed with C57BL/6 wild-type mice and genotyped by PCR of tail DNA using 5′-TTC CAC CAA AAT ATG GCC TCC AAT TTA CTG ACC GTA C-3′ (forward) and 5′-TCA ACC AGT TTA GTT ACC C-3′ (reverse). Dcx-CreER[T2] mice were crossed with the Z/EG reporter mice (Jackson Laboratory). Offspring carrying both transgenes were treated with injections of tamoxifen (250 mg per kg of body weight, T-5648, Sigma).

The Dcx-CreER[T2] mice have been characterized and express GFP in newly formed neurons in the cerebral cortex during development and in the adult in the SVZ, RMS and olfactory bulb, but not in the hippocampus. The number of cells that was labeled also correlates with the dose and duration of TMX injections. The Dcx-CreER mice have normal development without any noticeable phenotype as compared to their wild-type littermates.

LPC-induced demyelination. Demyelination was performed in adult (P40–60) GAD65-GFP, Dcx-GFP mice and Dcx-CreER[T2] mice after deep ketamine/xylazine anesthesia (10 mg per g body weight). Mice were placed in a stereotaxic frame (Stoelting) and 2 μl of 1% LPC solution (vol/vol) and/or 0.9% NaCl (vol/vol) was injected into the corpus callosum using Hamilton micropipettes (Stoelting). Injection time lasted 5 min to reduce reflux along needle track. Stereotaxic coordinates for corpus callosum were taken from the bregma (0.26 mm caudal, 1.0 mm lateral and 2.5 mm ventral). The day of injection was designated as day 0. At several time points (2, 5 and 10 dpl) after LPC and/or NaCl injections, mice were processed for cell culture or immunocytochemistry, or SVZ tissue was dissected for cell cultures. To permanently label cells in Dcx-CreER[T2] mice, we injected them with tamoxifen twice. The first injection was performed intraperitoneally 24 h before the LPC injection. LPC-induced demyelination was performed the next day and tamoxifen was injected again 24 h later.

Immunohistochemistry and cell counting. Floating brain sections from GAD65-GFP and Dcx-GFP mice or from LPC- or NaCl- injected GAD65-GFP, Dcx-GFP and Dcx-CreER[T2] mice, were immunostained with various antibodies to BrdU, Mash1, Olig2, CC1, Pax6, CNP, MBP, NG2, GFAP, NeuN, Doublecortin, Ki67, S100β, MAP2, GAD65/67, Nkx2.2 (Developmental Studies Hybridoma Bank, University of Iowa) and Dlx2 (gift from K. Yoshikawa, Osaka University). All antibody dilutions were previously described[14,49,50]. Sections were incubated overnight at 4 °C in primary antibodies diluted in 0.1 M phosphate-buffered saline (pH 7.4) containing 0.1% Triton X-100 (vol/vol) and 5% normal goat serum (vol/vol). For secondary antibodies, we used TRITC-conjugated AffiniPure goat antibody to mouse IgG, FITC-conjugated AffiniPure goat antibody to rabbit IgG and TRITC-conjugated AffiniPure goat antibody to mouse IgM. Sections were incubated with secondary antibodies for 1 h at 22–25 °C, then washed and mounted on slides. For cell counting, *z* stacks of 1-μm-thick single-plane images were captured through the entire thickness of the slice using a confocal microscope (MRC1024, BioRad Laboratories and Zeiss) and collapsed before cell counting. After images were collected, samples were stacked and analyzed using ImageJ (US National Institutes of Health). Measurements were taken from 15–20 tissue sections obtained from three to four mice per group. Cells were quantified using unbiased stereological morphometric analysis for the SVZ and corpus callosum to obtain an estimate of the total number of positive cells. Percentages and total number of cells expressing different antigens were estimated by scoring the number of cells double labeled with the marker(s) in question. Statistical significance was determined using Student's *t* test.

Transplantation and analysis of grafted cells. Wild-type P2 FVB/NxCB6 pups were used as recipients. FACS-purified GAD65-GFP–positive donor cells were prepared from the SVZ of P8 GAD65-GFP transgenic mice. Immediately after FACS sorting, cells were transplanted directly into the lateral ventricle of host brains as described previously[49]. For anatomical studies of grafted cells, mice were killed 5–8 d after transplantation and cells were immunostained as described above. Grafted GAD65-GFP–positive cells were readily visible without tissue manipulation under confocal microscopy using 488-nm laser-line excitation.

BrdU administration. The BrdU labeling protocol was previously described[49]. The number of proliferating progenitor cells in SVZ and in demyelinated corpus callosum was determined following short-term (2 h) or long-term (BrdU injection every 24 h for 5 consecutive days) incorporation. Mice were killed either 2 h or 2 d after the last BrdU injection. Brains were then sectioned for immunocytochemistry.

***In vivo* viral labeling.** SVZ cells were infected by direct injection of a retrovirus (CMV-dsRed) into the lateral ventricle. Retrovirus production and titer determination were as previously described[14]. P40–60 GAD65-GFP mice were injected with retrovirus stock (2 μl, titer of $2–4 \times 10^6$ cfu per ml). Virus injections were performed stereotaxically 2 d before LPC injections (relative to bregma, 0 mm anteroposterior, 1,8 mm mediolateral and 3.0 mm dorsoventral from brain surface). Brains were processed for histology at 2, 5 and 14 d after infection and sections were immunostained for Olig2, CC1, GFAP and S100β.

FACS purification of GFP-positive cells and cell cultures. SVZs were dissected from 300-μm-thick brain sections prepared from GAD65-GFP mice (P40) or from GAD65-GFP and Dcx-GFP mice (P40–60) after NaCl or LPC injection into the corpus callosum. Tissue was digested for 30 min at 37 °C in Hank's balanced salt solution containing papain (13 units per ml), DNAse (5 units per ml) and trypsin, and dissociated by trituration. Cells were resuspended in Hank's buffer containing 1 M HEPES, 15% sucrose (vol/vol) and penicillin/streptavidin. After washing with D-MEM/F12 medium, cells were FACS sorted as previously described[50] (Influx, Cytopeia). To sort GAD65-GFP–positive, NG2-positive cells, we labeled cells with antibody to NG2 for 1 h at 4 °C. Cells were then carefully washed in medium and incubated in the secondary antibody (RPE) for 1 h at 4 °C. Purified GAD65-GFP–positive, Dcx-GFP–positive, and GAD65-GFP–positive and NG2-positive cells were plated on 24-well dishes coated with poly-L-lysine at 10 cells per μl, and cultured in stem cell medium supplemented with 1% N2 (vol/vol) and 1% B27 (vol/vol) and Dulbecco modified eagle medium with penicillin and 10% fetal bovine serum (vol/vol). To study the effects of chordin on GAD65-GFP–positive and Dcx-GFP–positive cell development, we incubated FACS-sorted cells for 5 d in basal medium containing either VEGF (5 ng ml^{-1}) or chordin (6 μg ml^{-1}). To block the effects of chordin, we also cultured GAD65-GFP–positive cells under the same conditions with antibody to chordin (0.2 μg μl^{-1}) for 5 d. Mouse antibody to IgG was used as a control. Cultured GAD65-GFP–positive cells were immunolabeled with neuronal or glial markers or cells were harvested for RNA analysis. Standard protocols were used for immunohistochemistry of cultured GAD65-GFP–positive and Dcx-GFP–positive cells[50] with primary antibodies to GalC (galactocerebroside), MAP2, GFAP, Mash1, and Olig2.

RT-PCR. For RT-PCR, RNA was isolated from P40–60 SVZ tissue or from FACS-purified GAD65-GFP–positive cells from the SVZ, using Trizol. cDNA was first synthesized using the SuperScript First-Strand cDNA Synthesis kit with 1.5–2.0 µg of total RNA in a total volume of 11 µl, including 10 mM dNTP mix and 0.5 µg µl^{-1} Oligo dT. Reaction mixtures were heated at 65 °C for 5 min, then at 42 °C for 50 min. From 2 µl of cDNAs, sequences of interest were amplified in a thermocycler in a total volume of 25 µl of mixture with Tag polymerase. The mouse gene–specific primers were obtained from Integrated DNA Technologies (primer sequences for PCR analysis are listed in the RT-PCR section). Genes were amplified by denaturation at 94 °C for 1 min, annealing at 55 °C for 1 min, and extension at 72 °C for 1 min for 35 cycles. PCR products were resolved by 1.2% agarose gel electrophoresis and visualized by ethidium bromide staining. Band intensity was measured using ImageJ (US National Institutes of Health). GAD65: sense (5′-CCA TTA CCC CAA TGA GCT TCT-3′), antisense (5′-CCC CAA GCA GCA TCC ACG T-3′); MAP2: sense (5′-CAC CAG CCG TTT GAG AAT AC-3′), antisense (5′-GCT GTT TCT TCG GCT GCT AG-3′); Dlx2: sense (5′-GGC ACC AGT TCG TCT CCG GTC AA-3′), antisense (5′-CGC CGA AGT CCC AGG ATG CTG-3′); Mash1: sense (5′-GAA CTG ATG CGC TGC AAA C-3′), antisense (5′-TGG AGT AGT TGG GGG AGA TG-3′); Olig2: sense (5′-GTG TCT AGT CGC CCA TCG TC-3′), antisense (5′-CGA TGT TGA GGT CGT GCA T-3′); GFAP: sense (5′-ACT TAA CAA ATC CCT TCC TTC ATC C-3′), antisense (5′-CCC TCT CTC CTG TTT CAG TG-3′); Actin: sense (5′-CGT GGG CCG CCC TAG GCA CCA-3′), antisense (5′-TTG GCC TTA GGG TTC AGG GGG-3′).

Microarray and PCR analysis. GEArray expression array systems (cat#OMM031 SuperArray) consisted of spotted cDNA fragments encoding 113 mouse genes for neurotrophic signaling molecules involved in neuronal growth and differentiation, as well as regeneration and survival. Control sequences (PUC18, *Gapdh*, *Ppia* and *Actb*) were also included. These microarrays were employed to compare SVZ gene expression 4 d after NaCl or LPC injection in corpus callosum. Total RNA was isolated by Trizol (Invitrogen) and processed for microarray hybridization following the manufacturer's instructions. Arrays were visualized by autoradiography, and hybridization signals were scanned and analyzed for density in

GEArray Expression Analysis Suite 2.0. The normalized value for each gene was calculated by dividing the value of each gene by the average value of the house-keeping genes *Gapdh*, *Ppia* and *Actb*. To confirm microarray data, we used the following primers: ALK-3: sense (5′-TGT GGG TTG CAA ATA CTG GTT A-3′), antisense (3′-AAT CAG ACT CCG ACC AGA AAA A-5′); ALK3: sense (3′-CAG ACT TGG ACC AGA AGA AGC C-5′), antisense (5′-ACA TTC TAT TGT CTG CGT AGC-3′); ALK6: sense (3′-AAG AAG ATG ACT CTG GAA TGA A-5′), antisense (5′-ATC CAC ACC TCG CCA TAG CG-3′); Noggin: sense (3′-AAG GAT CTG AAC GAG ACG-5′), antisense (5′-GCA GGA ACA CTT ACA CTC G-3′); BMP2: sense (3′-CCA GGT TAG TGA CTC AGA ACA C-5′), antisense (5′-TCA TCT TGG TGC AAA GAC CTG C-3′); BMP-2: sense (5′-AGC AGG TGG GAA AGT TTT GA-3′), antisense (5′-CTC GTC AAG GTA CAG CAT CG-3′); BMP4: sense (3′-CTC CCA AGA ATC ATG GAC TG-5′), antisense (5′-AAA GCA GAG CTC TCA CTG GT-3′).

Osmotic minipumps infusion. We infused chordin, antibody to chordin (100 nm µl^{-1}, R&D systems, diluted in vehicle, 0.9% saline, vol/vol) or vehicle alone onto the lateral ventricle brain surface of adult GAD65-GFP and Dcx-GFP mice (infusion coordinates: anterioposterior, 0; lateral, 1.1; dorsoventral, 1.5 mm relative to bregma) 2 d after NaCl or LPC injections into corpus callosum for 5 d using micro-osmotic pumps (Alzet, model 1007) connected to a 30-gauge stainless-steel cannula through polyethylene catheter tubing (brain infusion kit, Durect). The flow rate of the pumps was 0.25 ± 0.02 µl h^{-1}, as determined by the supplier. The osmotic pump was inserted into a subcutaneous pocket below the neck, leading the catheter to the site for cannula placement. Mice were then killed by perfusion with 4% paraformaldehyde (vol/vol) and coronal brain sections (50 µm) were prepared for immunohistochemistry.

49. Aguirre, A.A., Chittajallu, R., Belachew, S. & Gallo, V. NG2-expressing cells in the subventricular zone are type C-like cells and contribute to interneuron generation in the postnatal hippocampus. *J. Cell Biol.* **165**, 575–589 (2004).
50. Aguirre, A., Rizvi, T.A., Ratner, N. & Gallo, V. Overexpression of the epidermal growth factor receptor confers migratory properties to nonmigratory postnatal neural progenitors. *J. Neurosci.* **25**, 11092–11106 (2005).